**Proceedings of the ASME 2021
International Design Engineering Technical Conferences and
Computers and Information in Engineering Conference
IDETC/CIE2021
August 17-20, 2021, Virtual, Online**

DETC2021-XXXXX

MULTIFIDELITY UNCERTAINTY QUANTIFICATION FOR ONLINE SIMULATIONS OF AUTOMOTIVE PROPULSION SYSTEMS

Hang Yang*
Department of Mechanical Engineering
University of Michigan
Ann Arbor, Michigan 48109

Alex Gorodetsky
Department of Aerospace Engineering
University of Michigan
Ann Arbor, Michigan 48109

Yuji Fujii
Research and Advanced Engineering
Ford Motor Company
Dearborn, Michigan 48124

Kon-Well Wang
Department of Mechanical Engineering
University of Michigan
Ann Arbor, Michigan 48109

ABSTRACT

The increasing complexity and demanding performance requirement of modern automotive propulsion systems necessitate more intelligent and robust predictive controls. Due to the significant uncertainties from both unavoidable modeling errors and probabilistic environmental disturbances, the ability to quantify the effect of these uncertainties to the system behaviors is of crucial importance to enable advanced control designs for automotive propulsion systems. Furthermore, the quantification of uncertainty must be computationally efficient such that it can be conducted in real-time on board a vehicle. However, traditional uncertainty quantification methods for complicated nonlinear systems, such as Monte Carlo, often rely on sampling — a computationally prohibitive process for many applications. Previous research has shown promises of using spectral decomposition methods such as generalized polynomial chaos to reduce the online computational cost of uncertainty quantification. However, such method suffers from scalability and bias issues. This paper seeks to alleviate these computational bottlenecks by developing a multifidelity uncertainty quantification method that combines low-order generalized polynomial chaos with Monte Carlo estimation via Control Variates. Results on the mean and variance estimates of the axle shaft torque show that the proposed method can correct the bias of low-order PCE expansions while significantly reducing variance compared to pure Monte Carlo.

INTRODUCTION

Robust online simulations are of great importance in enabling predictive control in many automotive systems. This capability is especially valuable for optimizing performance, efficiency, durability, and safety of advanced automotive propulsion systems with complicated system configurations and the complex interactions between components. Unfortunately, high-fidelity models that capture detailed system behaviors are often too computationally expensive to run on-board a vehicle for control purposes in real-time. On the other hand, simplified models often introduce errors and uncertainties that sacrifice the reliability of the simulation outcomes. Past research efforts have shed light upon the challenges in balancing model fidelity and computational efficiency for real-time simulations of automotive propulsion systems [1–4], most of which use simplified deterministic propulsion system models. However, there are signif-

*Address all correspondence to this author at hangyang@umich.edu.

icant uncertainties in these models due to the complex behaviors of the hydro-mechanical components, such as torque converters and wet clutches, that cannot be fully captured in simplified deterministic models. Furthermore, significant uncertainties in driver inputs and environmental disturbances are unavoidable. These uncertainties essentially render the systems stochastic. To address the stochastic nature of the system, this paper adopts a stochastic model formulation proposed in [5] that directly accounts for various model uncertainties and random driver behaviors. The stochastic model is used to achieve robust online simulations of a typical automotive propulsion system [6]. Uncertainty quantification (UQ) methods are applied to efficiently and accurately conduct and assess the simulations of the stochastic model.

Uncertainty quantification of complicated nonlinear systems can cause significant computational burden as closed-form solutions to the stochastic system dynamics often do not exist. To address the UQ of this class of systems, multiple approaches have been developed in the literature. These approaches can be categorized into two families of methods: the *sampling* methods and *non-sampling* methods. Sampling methods, such as the Monte Carlo (MC) and its variants [7, 8], are based on solving an ensemble of realizations of the stochastic systems. These methods are generally very flexible and easy to apply to a wide range of systems. However, the convergence rate is typically low, which leads to high computational cost in many applications.

Non-sampling methods, on the other hand, do not depend on drawing samples from the distributions of underlying random variables. These methods often explore the system structures and apply approximations to estimate statistical quantities of interest. Classic examples of non-sampling methods include perturbation methods [9] and stochastic operator methods [10]. However, these methods are often limited to either systems with specific types of governing equations and/or systems under low levels of uncertainties. To address these limitations, recent efforts in the literature have focused on developing algorithms using generalized Polynomial Chaos (gPC), a spectral-decomposition-based approach for approximating the statistical moments of random variables in stochastic systems [11–15]. For estimating smooth quantities of interests, gPC can be very accurate and fast. Specifically, the efficacy of using gPC for UQ in online simulations of automotive propulsion systems in certain operating scenarios was studied in [5]. However, the computational cost of applying gPC grows exponential with increasing system dimension. As a result, practical applications of gPC are often restricted to low-degree PC expansions, which unavoidably introduces biases in the UQ estimates.

Hence, this research aims to answer the important research question of whether a small amount of MC samples could alleviate the inherent scalability and bias issues of gPC. Specifically, investigations are focused on fusing gPC with MC in a multifidelity framework to correct the gPC bias without introducing significant variance. In computational science and engineering, multifidelity techniques have a long and successful history in leveraging models at different fidelity levels to achieve more efficient computation for a given accuracy [16–20]. For UQ methods that employ sampling techniques such as MC, multifidelity methods seek to reduce the estimator variance. With a lower estimator variance, fewer samples are needed to achieve certain estimation accuracy, leading to a reduced computational cost.

Control Variates (CV) [7, 21–24], a powerful multifidelity framework, is adopted in this research to combine gPC and MC for unbiased and low-variance estimation. CV introduce additional estimators based on low-fidelity models that are correlated with the original estimator with a high-fidelity model, and has seen a recent resurgence for UQ problems where the high-fidelity models can be expensive to evaluate [25, 26]. Recent efforts in the literature have shown promising results of using gPC in CV as a means of achieving more efficient UQ [27–29]. However, none one these early attempts of such approach has studied its application and efficacy in predictive simulations of dynamic systems.

The goal of this research is to advance the state of the art through investigations of the feasibility and efficacy of a CV-based multifidelity framework that combines gPC and MC in the UQ for online simulations of automotive propulsion systems. The remainder of the paper is organized as follows. A system model suitable for online simulations is developed. Then, the formulation of the proposed multifidelity UQ method is derived and its main properties are discussed. Application results of the proposed method in the problem of interest is then presented, followed by discussions and conclusions.

SYSTEM MODEL

This paper considers the propulsion system of a conventional vehicle equipped with a internal combustion engine and a 10-speed automatic transmission [5]. Note that the method developed in this work can also be adopted by vehicles with hybrid propulsion systems. Fig. 1 shows the components of the propulsion system. The operating scenario of a vehicle launch in first gear is studied as an example.

Assume rigid body dynamics and treat engine torque demand as an idealized torque source, the equation of motion of the engine is:

$$I_e \dot{\omega}_e = (1 - r_e)\tau_e - \tau_{im} \tag{1}$$

where I_e, ω_e, and τ_e are the effective moment of inertia, angular speed, and torque of the engine, respectively; r_e is the engine torque reduction ratio; τ_{im} is the reaction torque of the impeller of the torque converter. To capture the naturally probabilistic

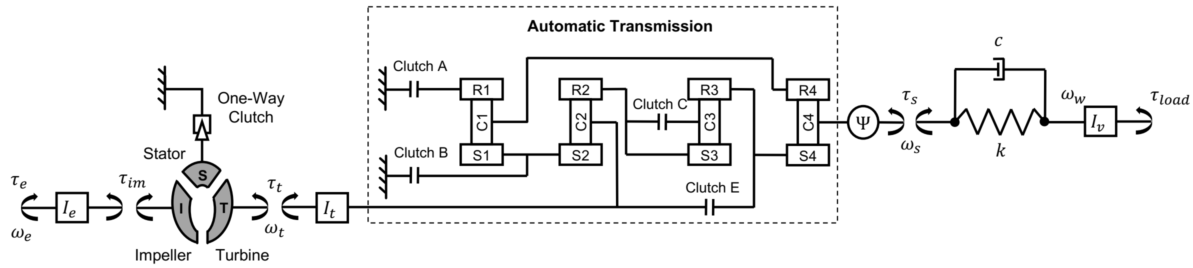

FIGURE 1. Schematic of an automotive propulsion system with a torque convert and a step-ratio automatic transmission. [5]

behavior of the driver, the engine torque demand in Eqn. (1) is modeled as a linear function with an probabilistic uncertain parameter:

$$\tau_e = ut + u_0 \tag{2}$$

where u_0 is the initial engine torque demand and u is the rate of change of engine torque demand modeled as a Gaussian random variable such that $u \sim \mathcal{N}(\mu_u, \sigma_u)$, where μ_u and σ_u are the mean and standard deviation of u.

The torque converter in Fig. 1 enables hydrodynamic torque multiplication during vehicle launch and provides torsional vibration absorption between the engine and the drivetrain [30]. Simulations that describe the detailed dynamics of the torque converter require expensive computational fluid dynamics (CFD) models, which are not feasible for on-board applications in a vehicle. In this paper, a simplified model for the steady-state dynamics of the torque converter with locked stator [31] is adopted:

$$\tau_{im} = a_0\omega_{im}^2 + a_1\omega_{im}\omega_t + a_2\omega_t^2 \tag{3}$$

$$\tau_t = b_0\omega_{im}^2 + b_1\omega_{im}\omega_t + b_2\omega_t^2 \tag{4}$$

where ω_{im} is the angular velocity of the torque converter impeller; ω_t and τ_t are the torque converter turbine angular speed and torque, respectively; a_0, a_1, a_2, b_0, b_1, and b_2 are constants that can be estimated using test data [6].

During a vehicle launch in first gear, Clutch A, B, and E are engaged. As vehicle gains speed, the automatic transmission starts the gear shifting procedure, which involves controlling wet clutches to achieve a smooth sway of torque path from Clutch E to Clutch C. This research only considers system dynamics up until the first phase of this torque swap procedure, namely the torque phase.

Downstream from the automatic transmission, propulsion torque is transmitted to the drive wheels via the driveline:

$$I_v\dot{\omega}_r = \tau_s - \tau_{load} \tag{5}$$

where I_v is the effective moment of inertia of the vehicle at drive wheels; ω_w is the angular speed of the drive wheels; τ_s is the axle shaft torque; and τ_{load} is the load torque exerted on the vehicle through the drive wheels.

Assuming zero backlash in the drivetrain, the axle shaft torque can be expressed as:

$$\tau_s = k(\theta_s - \theta_w) + c(\omega_s - \omega_w) \tag{6}$$

where k and c are the lumped stiffness and damping in the drivetrain modeled as Gaussian random variables to capture the model parametric uncertainty of the drivetrain such that $k \sim \mathcal{N}(\mu_k, \sigma_k)$ and $c \sim \mathcal{N}(\mu_c, \sigma_c)$; θ_s and θ_r are angular displacements of the axle shaft and drive wheels; ω_s and ω_r are angular velocities of the axle shaft and drive wheels.

Given the dynamics of the subsystems, the overall equation of motion of the system in FIGURE 1 in the aforementioned operating scenario can be summarized as follows:

$$\dot{\omega}_e = C_{11}\tau_e + C_{12}\omega_e^2 + C_{13}\omega_e\omega_s + C_{14}\omega_s^2 \tag{7}$$

$$\dot{\omega}_s = C_{21}\omega_e^2 + C_{22}\omega_e\omega_s + C_{23}\omega_s^2 + C_{24}\tau_C + C_{25}\tau_s \tag{8}$$

$$\dot{\omega}_w = C_{31}\tau_s + C_{32}\omega_w^2 + C_{33} \tag{9}$$

$$\begin{aligned}\dot{\tau}_s = {} & C_{41}\omega_s + C_{42}\omega_w + C_{43}\omega_s^2 + C_{44}\omega_e\omega_s + \\ & C_{45}\omega_s^2 + C_{46}\tau_C + C_{47}\tau_s + C_{48}\omega_w^2 + C_{49}\end{aligned} \tag{10}$$

where τ_C is the torque capacity of Clutch C and C_{ij} are lumped coefficients similar to the formulations described in [6]. The dynamics of wet clutch is highly nonlinear. Furthermore, torque generation of wet clutches is affected by many factors that depend on specific operating conditions [32]. Clutch torque capacity predictions given by control-oriented models often come with considerable uncertainty. To account for the uncertainty, the torque capacity of Clutch C is modeled as follows:

$$\tau_C = \bar{\tau}_C + \lambda_C \tag{11}$$

where $\bar{\tau}_C$ is the predicted torque capacity and $\lambda_C \sim \mathcal{N}(\mu_{\lambda_C}, \sigma_{\lambda_C})$ is an uncertain offset from the predicted values.

Multifidelity Uncertainty Quantification Using Control Variates and Generalized Polynomial Chaos

This section describes the proposed method that combines the sampling method MC and the non-sampling spectral decomposition method gPC via a CV framework to achieve highly efficient and yet flexible UQ with guaranteed unbiased estimations.

Monte Carlo and Control Variates. Let $Q : \mathbb{R}^d \to \mathbb{R}$ be a random variable mapping from a vector of inputs to a scalar valued output. Q is referred to as the high-fidelity model as it represents the stochastic process of interest exactly. The MC estimate of the mean $\mu = \mathbb{E}[Q]$ using a samples $\boldsymbol{\xi} = \left(\xi^{(1)}, \xi^{(2)}, \cdots, \xi^{(N)}\right)$ is:

$$\hat{Q}^{MC}(\xi) = \frac{1}{N}\sum_{i=1}^{N} Q\left(\xi^{(i)}\right) \tag{12}$$

The MC-based linear CV introduces an additional random variables Q_1 with a known mean μ_1. This new random variable represents the solution to a low-fidelity model of the same system. Then, CV requires computing another estimate $\hat{Q}_1^{MC}$ of μ_1 using the same samples that were used in $\hat{Q}^{MC}$. By leveraging estimates from both the high and low-fidelity models in the following way, CV can achieve a lower overall variances for the CV estimator:

$$\hat{Q}^{CV}(\alpha, \boldsymbol{\xi}) = \hat{Q}^{MC}(\boldsymbol{\xi}) + \alpha\left(\hat{Q}_1^{MC}(\boldsymbol{\xi}) - \mu_1\right) \tag{13}$$

where α is a design parameter called CV weight. The low fidelity estimator $\hat{Q}_1^{MC}$ is also referred to as the Correlated Mean Estimator (CME). The know mean of the lower-fidelity mode is referred to as the Control Variate Mean (CVM).

Denote the optimal CV weight α^*, then:

$$\alpha^* = \arg\min_{\alpha} \mathbb{V}ar\left[\hat{Q}^{CV}\right] \tag{14}$$

where $\mathbb{V}ar\left[\hat{Q}^{CV}\right] = \mathbb{V}ar\left[\hat{Q}^{MC}\right] + \alpha^2\mathbb{V}ar\left[\hat{Q}_1^{MC}\right] + 2\alpha\mathbb{C}ov\left[\hat{Q}^{MC}, \hat{Q}_1^{MC}\right]$. The corresponding optimal estimator variance is:

$$\mathbb{V}ar\left[\hat{Q}^{CV}(\alpha^*)\right] = \mathbb{V}ar\left[\hat{Q}^{MC}\right](1-\rho^2) \tag{15}$$

where $\rho \in [-1, 1]$ is the Pearson correlation coefficient between $\hat{Q}^{MC}$ and $\hat{Q}_1^{MC}$.

As shown in Eq. (15), the maximum variance reduction is achieved when the high-fidelity model and low-fidelity model are perfectly correlated, meaning $\rho = 1$. On the other hand, there is no variance reduction over the standard MC estimator if the low-fidelity model has no correlation with the high-fidelity model. Therefore, when designing CV estimators, it is important to select low-fidelity models that are as correlated as the high-fidelity model as possible.

Generalized Polynomial Chaos. For a dynamic system governed by a set of ordinary different equations system with states $\mathbf{x} \in \mathbb{R}^{n_x}$, control inputs $\mathbf{u} \in \mathbb{R}^{n_u}$, and uncertain parameters represented as a set of random variables $\boldsymbol{\xi} \in \mathbb{R}^{n_\xi}$, the general equations of motion is:

$$\dot{\mathbf{x}}(t, \boldsymbol{\xi}) = f\left(\mathbf{x}(t, \boldsymbol{\xi}), \mathbf{u}(t, \boldsymbol{\xi}), t, \boldsymbol{\xi}\right) \tag{16}$$

where $f : \mathbb{R}^{n_x} \times \mathbb{R}^{n_u} \times \mathbb{R}^{n_\xi} \to \mathbb{R}^{n_x}$. Instead of drawing samples from the probability distribution of the uncertain parameters $\boldsymbol{\xi}$, gPC utilizes spectral approximation to decompose the system and expresses the solution to Eqn. (16) as orthogonal polynomials of the input random variables defined on a given probability space:

$$\mathbf{x}(t, \boldsymbol{\xi}) = \sum_{i=0}^{\infty} x_i(t)\boldsymbol{\Phi}_i(\boldsymbol{\xi}) \tag{17}$$

where $x_i(t)$ is a set of deterministic PC coefficients that are functions of time and $\boldsymbol{\Phi}_i(\boldsymbol{\xi})$ are a set of polynomial bases that satisfies the orthogonality condition $\int_S \Phi_n(\boldsymbol{\xi})\Phi_m(\boldsymbol{\xi})w(\boldsymbol{\xi})d\boldsymbol{\xi} = \gamma_n\delta_{mn}, \forall m, n \in \{0, 1, \cdots, M-1\}$ with respect to a probability measure β, where S is the support of β, $w(\boldsymbol{\xi})$ is the density of β, $\gamma_n = \int_S \Phi_n^2(\boldsymbol{\xi})w(\boldsymbol{\xi})d\boldsymbol{\xi}$ is a normalization constant, and δ_{mn} is a Kronecker delta function that is equal to 1 when $m = n$ and zero otherwise.

The expansion in Eq. 17 is exact. However, PC with infinite number of terms is not practical. Therefore, an estimate of Eq. 17 is obtained by truncate the PC at a finite degree:

$$\hat{\mathbf{x}}(t, \boldsymbol{\xi}) = \sum_{i=0}^{M-1} \hat{x}_i(t)\boldsymbol{\Phi}_i(\boldsymbol{\xi}) \tag{18}$$

where $M = \frac{(p+n_\xi)!}{n_\xi!\,p!}$ is total number of terms in the PC expansion and p is the degree at which the PC expansion is truncated. If $\mathbf{x}(t, \boldsymbol{\xi})$ has bounded variance, the approximate in Eqn. (18) converges exponentially in the L_2 sense.

In this paper, gPC is used in an intrusive manner to construct the equation of motion for the PC coefficients directly. Specifically, the expansion in Eqn. (18) is applied to the general system defined in Eqn. (16) to give the equation of motion of the system with respect to the polynomial bases. Then, the stochastic Galerkin projection technique is used to project the expansion onto each of the polynomial bases $\{\mathbf{\Phi}_i(\boldsymbol{\xi})\}$, forcing the approximation error to be orthogonal to the functional space spanned by the basis polynomials. The outcome is a set of deterministic equations that describes the estimated dynamics of the PC coefficients:

$$\frac{d\hat{x}_i(t)}{dt} = \frac{\langle f, \mathbf{\Phi}_i(\boldsymbol{\xi})\rangle}{\langle \mathbf{\Phi}_i^2(\boldsymbol{\xi})\rangle} \tag{19}$$

Then, the statistical moment estimates, such as mean and variance, can be retrieved from the solution of Eqn. (19) with minimal computational cost:

$$\hat{\mu}(t) = \hat{x}_0(t) \tag{20}$$

$$\hat{\sigma}^2(t) = \sum_{i=1}^{M-1} \hat{x}_i^2(t) \tag{21}$$

As the result in Eqn. (19) contains $M-1$ coupled deterministic ordinary differential equations, the number of coupled equations that one needs to solve in order to resolve the dynamics of the PC coefficients grows rapidly with the number of input random variables n_ξ and the truncation degree p. Therefore, in most real-world applications, PC expansions are truncated at very low degree of expansion to avoid the rapidly increasing computational cost. The necessity to keep the truncation degree low unavoidably bring biases in the estimates for UQ.

Control Variate Polynomial Chaos (CVPC). In this section, a multi-fidelity UQ method that combines gPC and MC using the CV framework is derived. This proposed method explores synergies between gPC and MC by using samples of PC expansion bases and deterministic gPC coefficients to estimate CME while using the analytical solution from gPC to obtain CVM. The outcome is a method that combines the efficiency of gPC and the flexibility of MC while guaranteeing unbiased estimates.

Let $\boldsymbol{\xi}$ be a set of random variables with finite variances and probability distributions that is known or can be estimated. Transformation can be done to include system-dependent statistical characteristics in $\boldsymbol{\xi}$. Then the CV estimator introduced in Eqn. (13) can be modified to incorporate a gPC model as the low-fidelity model, giving the one-level CVPC estimator:

$$\hat{Q}^{CVPC}(\alpha, \boldsymbol{\xi}) = \hat{Q}^{MC}(\boldsymbol{\xi}) + \alpha\left(\hat{Q}^{MC}_{PC}(\boldsymbol{\xi}) - \hat{\mu}\right) \tag{22}$$

where $\hat{Q}^{MC}$ is a MC estimator using the high-fidelity model Q, $\hat{Q}^{MC}_{PC}(\boldsymbol{\xi})$ is a MC estimator that samples the bases of the PC expansion in a gPC estimator $\hat{Q}^{gPC}(t, \boldsymbol{\xi})$, and $\hat{\mu}$ is the analytical mean obtained using gPC. The gPC estimator $\hat{Q}^{gPC}(t, \boldsymbol{\xi})$ follows the expansion in Eqn. (18). $\hat{Q}^{MC}_{PC}(\boldsymbol{\xi})$ then estimates $\hat{Q}^{gPC}(t, \boldsymbol{\xi})$ by sampling the bases $\mathbf{\Phi}_i(\boldsymbol{\xi})$. Because of the fact that $Q^{MC}(\boldsymbol{\xi})$ and $Q^{MC}_{PC}(\boldsymbol{\xi})$ share the same underlying random variable and the fact that the PC expansion is based on the high-fidelity model Q, the two random variables are highly correlated. As shown in Eqn. (15), this high correlation will produce large variance reduction for the CVPC estimator.

Let the true mean of Q be μ, then the expectation of $\hat{Q}^{CVPC}(\alpha, \boldsymbol{\xi})$ can be written as:

$$\mathbb{E}\left[\hat{Q}^{CVPC}(\alpha, \boldsymbol{\xi})\right] = \mathbb{E}\left[\hat{Q}^{MC}(\boldsymbol{\xi})\right] + \alpha\mathbb{E}\left[\hat{Q}^{MC}_{PC}(\boldsymbol{\xi}) - \hat{\mu}\right] \tag{23}$$

Because MC estimators are unbiased, the CME and CVM in Eqn. 23 cancel out, yielding an unbiased estimator:

$$\mathbb{E}\left[\hat{Q}^{CVPC}(\alpha, \boldsymbol{\xi})\right] = \mu \tag{24}$$

Given a pair of high-fidelity MC and low-fidelity gPC estimators, the estimator variance of CVPC is a quadratic function with respect to the CV weight α. Therefore, the optimal CV weight is:

$$\alpha^* = -\frac{\mathbb{C}ov\left[\hat{Q}^{MC}(\boldsymbol{\xi}), \hat{Q}^{MC}_{PC}(\boldsymbol{\xi})\right]}{\mathbb{V}ar\left[\hat{Q}^{MC}_{PC}(\boldsymbol{\xi})\right]} \tag{25}$$

The corresponding estimator variance of CVPC is:

$$\mathbb{V}ar\left[\hat{Q}^{CVPC}(\alpha^*, \boldsymbol{\xi})\right] = \mathbb{V}ar\left[\hat{Q}^{MC}(\boldsymbol{\xi})\right](1-\rho^2) \tag{26}$$

where ρ is the Pearson correlation coefficient between the high-fidelity MC and low-fidelity gPC estimators.

RESULTS AND DISCUSSIONS

The proposed CVPC estimator in Eqn. (23) is applied to the automotive propulsion system in a vehicle launch simulation. Specifically, the lumped stiffness, lumped damping, and the rate of change in engine torque demand have standard deviations that are 20% of their respected nominal values. A $10Nm$ standard deviation is assigned to the on-coming clutch capacity offset.

A CVPC estimator using a degree-1 gPC and 10^2 MC samples of the high-fidelity model is implemented to obtain mean and variance estimates for the axle shaft torque. The result is

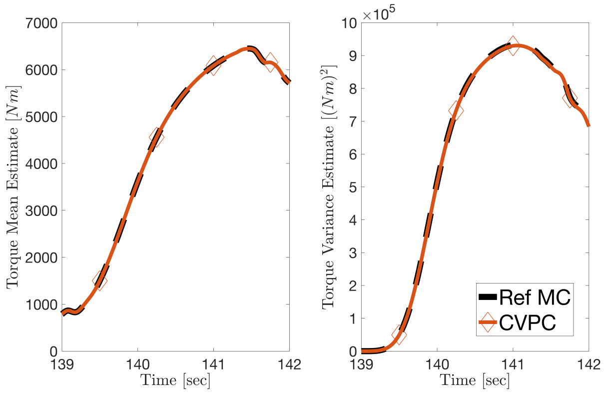

FIGURE 2. Average mean and variance estimates of the axle shaft torque obtained from 10^4 simulation experiments using CVPC. The CVPC estimator with 10^2 MC samples and a degree-1 gPC. The result is compared to the reference solution obtained using a MC estimator with a sample size of 10^6. The CVPC delivers average estimates that matches the reference solution, indicating that CVPC provides unbiased estimation.

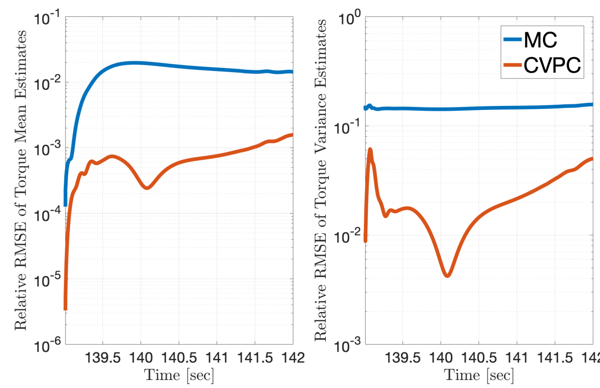

FIGURE 3. Comparisons between the relative RMSE of the CVPC estimator and that of a MC estimator under the same computational budget. The CVThePC estimator delivers significantly more accurate UQ compared to the MC estimator.

compared to a reference solution obtained using a MC estimator with 10^5 samples. As shown in Fig. 2, the average CVPC mean and variance estimates of the axle shaft torque calculated from 10^4 simulation experiments match the reference solution, which indicates the CVPC estimates are unbiased.

The online computational cost of running a CVPC estimator consists of three parts: a one-time cost for solving for the deterministic gPC coefficients; a negligible cost for sampling the polynomial bases; and the cost for solving the equations of motion for a small amount of MC sample. In comparison, a MC estimator often would need orders of magnitude more samples to achieve a desirable estimation accuracy, which results in significantly larger online computational cost. The efficiency advantage of CVPC is illustrated in Fig. 3 by comparing the relative root mean square errors (RMSE) of the estimates to that of a MC estimator under the same computational budget. As shown in Fig. 3, CVPC delivers significantly more accurate estimates compared to the MC estimator given a fixed computational cost. This efficiency gain is a result of the significant estimator variance reduction effect that CVPC brings. Furthermore, if an accuracy target is given, the estimator variance reduction effect would allow CVPC to achieve significantly faster computational than a MC estimator.

CONCLUSIONS

This paper proposes an efficient multifidelity UQ on method that combines a traditional MC estimator with a gPC estimator via the variance reduction framework of CV. The efficacy of the proposed method is demonstrated through the task of estimating mean and variance of the state variables of an automotive propulsion system during a vehicle launch. Through the simulation study and computational cost analysis, it is shown that the proposed CVPC method delivers significantly, in some cases of orders of magnitudes, more efficient UQ, compared to MC. Furthermore, the CVPC construction guarantees unbiased estimates, addressing the inherent biasing effect of gPC. Overall, the proposed method indicates significant potentials in delivering highly efficient uncertainty quantification for automotive propulsion systems and others with similar attributes. Future work to extend the CVPC method include investigating the optimal estimator design, the adoption of non-intrusive gPC as the low-fidelity model, and application of CVPC to stochastic control systems and reinforcement learning problems.

ACKNOWLEDGMENT

This research was supported by the Ford Motor Company.

REFERENCES

[1] Fathy, H. K., Filipi, Z. S., Hagena, J., and Stein, J. L., 2006. "Review of hardware-in-the-loop simulation and its prospects in the automotive area". In Modeling and simulation for military applications, Vol. 6228, International Society for Optics and Photonics, p. 62280E.

[2] Wang, L., Zhang, Y., Yin, C., Zhang, H., and Wang, C., 2012. "Hardware-in-the-loop simulation for the design and verification of the control system of a series–parallel hybrid electric city-bus". *Simulation Modelling Practice and Theory*, ***25***, pp. 148–162.

[3] Bachinger, M., Stolz, M., and Horn, M., 2015. "A novel

drivetrain modelling approach for real-time simulation". *Mechatronics,* ***32***, pp. 67–78.

[4] Shui, H., Zhang, Y., Yang, H., Upadhyay, D., and Fujii, Y., 2021. Machine learning approach for constructing wet clutch torque transfer function. Tech. rep., SAE Technical Paper.

[5] Yang, H., Kidambi, N., Fujii, Y., Gorodetsky, A., and Wang, K.-W., 2020. "Uncertainty quantification using generalized polynomial chaos for online simulations of automotive propulsion systems". In 2020 American Control Conference (ACC), IEEE, pp. 295–300.

[6] Yang, H., Kidambi, N., Wang, K.-W., Pietron, G. M., Hippalgaonkar, R., and Fujii, Y., 2019. Quantifying the effect of initialization errors for enabling accurate online drivetrain simulations. Tech. rep., SAE Technical Paper.

[7] Robert, C., and Casella, G., 2013. *Monte Carlo statistical methods*. Springer Science & Business Media.

[8] Giles, M. B., 2015. "Multilevel monte carlo methods.". *Acta Numer.,* ***24***, pp. 259–328.

[9] Liu, W. K., Belytschko, T., and Mani, A., 1986. "Probabilistic finite elements for nonlinear structural dynamics". *Computer Methods in Applied Mechanics and Engineering,* ***56***(1), pp. 61–81.

[10] Yamazaki, F., Shinozuka, M., and Dasgupta, G., 1988. "Neumann expansion for stochastic finite element analysis". *Journal of engineering mechanics,* ***114***(8), pp. 1335–1354.

[11] Xiu, D., and Karniadakis, G. E., 2002. "The wiener–askey polynomial chaos for stochastic differential equations". *SIAM journal on scientific computing,* ***24***(2), pp. 619–644.

[12] Xiu, D., 2010. *Numerical methods for stochastic computations: a spectral method approach*. Princeton university press.

[13] Ghanem, R., Higdon, D., and Owhadi, H., 2017. *Handbook of uncertainty quantification*, Vol. 6. Springer.

[14] Bavdekar, V. A., and Mesbah, A., 2016. "A polynomial chaos-based nonlinear bayesian approach for estimating state and parameter probability distribution functions". In 2016 American Control Conference (ACC), IEEE, pp. 2047–2052.

[15] Ernst, O. G., Mugler, A., Starkloff, H.-J., and Ullmann, E., 2012. "On the convergence of generalized polynomial chaos expansions". *ESAIM: Mathematical Modelling and Numerical Analysis,* ***46***(2), pp. 317–339.

[16] Ng, L. W.-T., 2013. "Multidelity approaches for design under uncertainty". PhD thesis, Massachusetts Institute of Technology.

[17] Peherstorfer, B., Willcox, K., and Gunzburger, M., 2018. "Survey of multifidelity methods in uncertainty propagation, inference, and optimization". *Siam Review,* ***60***(3), pp. 550–591.

[18] Geraci, G., Eldred, M. S., and Iaccarino, G., 2017. "A multifidelity multilevel monte carlo method for uncertainty propagation in aerospace applications". In 19th AIAA Non-Deterministic Approaches Conference, p. 1951.

[19] Goh, J., Bingham, D., Holloway, J. P., Grosskopf, M. J., Kuranz, C. C., and Rutter, E., 2013. "Prediction and computer model calibration using outputs from multifidelity simulators". *Technometrics,* ***55***(4), pp. 501–512.

[20] Peherstorfer, B., Willcox, K., and Gunzburger, M., 2016. "Optimal model management for multifidelity monte carlo estimation". *SIAM Journal on Scientific Computing,* ***38***(5), pp. A3163–A3194.

[21] Lavenberg, S. S., and Welch, P. D., 1981. "A perspective on the use of control variables to increase the efficiency of monte carlo simulations". *Management Science,* ***27***(3), pp. 322–335.

[22] Nelson, B. L., 1987. "On control variate estimators". *Computers & Operations Research,* ***14***(3), pp. 219–225.

[23] Emsermann, M., and Simon, B., 2002. "Improving simulation efficiency with quasi control variates".

[24] Geraci, G., Eldred, M., and Iaccarino, G., 2015. "A multifidelity control variate approach for the multilevel monte carlo technique". *Center for Turbulence Research Annual Research Briefs*, pp. 169–181.

[25] Geraci, G., Eldred, M. S., Gorodetsky, A., and Jakeman, J., 2019. "Recent advancements in multilevel-multifidelity techniques for forward uq in the darpa sequoia project". In AIAA Scitech 2019 Forum, p. 0722.

[26] Gorodetsky, A. A., Geraci, G., Eldred, M. S., and Jakeman, J. D., 2020. "A generalized approximate control variate framework for multifidelity uncertainty quantification". *Journal of Computational Physics,* ***408***, p. 109257.

[27] Garg, S., Sood, N., and Sarris, C. D., 2015. "Uncertainty quantification of ray-tracing based wireless propagation models with a control variate-polynomial chaos expansion method". In 2015 IEEE International Symposium on Antennas and Propagation & USNC/URSI National Radio Science Meeting, IEEE, pp. 1776–1777.

[28] Gu, Z., and Sarris, C. D., 2015. "Multi-parametric uncertainty quantification with a hybrid monte-carlo/polynomial chaos expansion fdtd method". In 2015 IEEE MTT-S International Microwave Symposium, IEEE, pp. 1–3.

[29] Fox, J., 2020. "Applications of polynomial chaos to monte carlo simulation". PhD thesis, The Florida State University.

[30] Hrovat, D., and Tobler, W., 1985. "Bond graph modeling and computer simulation of automotive torque converters". *Journal of the Franklin institute,* ***319***(1-2), pp. 93–114.

[31] Kotwicki, A. J., 1982. "Dynamic models for torque converter equipped vehicles". *SAE Transactions*, pp. 1595–1609.

[32] Fujii, Y., Kapas, N., and Tseng, J.-W., 2014. "Clutch wet". *Encyclopedia of Automotive Engineering*, pp. 1–15.

